Available online at www.sciencedirect.com

ScienceDirect

Mendeleev Commun., 2024, **34**, 418–420

Mendeleev Communications

A naphthalimide-based fluorescent and colorimetric probe for the detection of mercury(II) ions in aqueous solutions and in living cells

Anna S. Polyakova,*[a] Pavel A. Panchenko,[a,b] Anastasija V. Efremenko,[c] Alexey V. Feofanov,[c,d] Yuri V. Fedorov[a] and Olga A. Fedorova[a,b]

[a] *A. N. Nesmeyanov Institute of Organoelement Compounds, Russian Academy of Sciences, 119334 Moscow, Russian Federation. E-mail: ania.poliakova@mail.ru*
[b] *D. I. Mendeleev University of Chemical Technology of Russia, 125047 Moscow, Russian Federation*
[c] *M. M. Shemyakin–Yu. A. Ovchinnikov Institute of Bioorganic Chemistry, Russian Academy of Sciences, 117997 Moscow, Russian Federation*
[d] *Department of Biology, M. V. Lomonosov Moscow State University, 119234 Moscow, Russian Federation*

DOI: 10.1016/j.mencom.2024.04.034

A novel derivative of 4-styryl-1,8-naphthalimide containing an *N*-arylazadithia-15-crown-5-ether moiety as a receptor exhibited a hypsochromic shift with simultaneous fluorescence quenching upon complexation with the mercury(II) cation. The compound is suggested as a selective fluorescent chemosensor for the detection of Hg^{2+} in aqueous solutions and in HEK 293 cells.

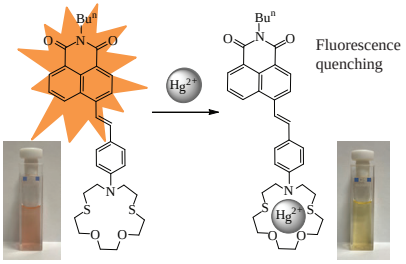

Keywords: sensor, mercury cation, fluorescence imaging, HEK 293 cells, intramolecular charge transfer, hypsochromic shift, azadithia-crown compounds, 1,8-naphthalimide, Heck reaction.

The development of selective and sensitive methods for determining heavy and transition-metal cations in aqueous solutions is currently attracting a considerable attention. Despite the fact that some cations of d-elements are involved in physiological processes occurring in body and are contained in some enzymes with various types of action,[1] they manifest toxic effects in the vast majority of cases, even at low concentrations.[2]

Mercury is among the most toxic heavy metals and it is widely distributed in the environment as a result of human activities. Mercury(II) ions are easily converted by marine microorganisms to methylmercury ($MeHg^+$) that is more harmful than inorganic or elemental mercury.[3] Further up the food chain,[4] $MeHg^+$ can accumulate in commercial fish, posing a threat to the human health. The extreme toxicity of mercury compounds is due to their high affinity to thiol groups of proteins and enzymes,[5] which causes cell dysfunction and thereby causes damage to the digestive, cardiovascular and central nervous systems.[6] Mercury poisoning can cause a variety of serious diseases, such as tremors, deafness, arthritis, loss of muscle coordination and memory, and movement disorders.

Based on the above, the qualitative and quantitative analysis of mercury cations in solutions and in cells of living organisms is currently an important concern. This problem is often solved using organic fluorescent reagents capable of changing the maximum wavelength and intensity of the band in the emission spectrum upon binding to metal ion.[7] Derivatives of 1,8-naphthalimide are among the most popular optical platforms for the creation of such reagents (fluorescent chemosensors).[8] Luminophores of this type have high thermal resistance and photostability, intense absorption and fluorescence in the visible region of the spectrum. Moreover, their photophysical properties can be finely tuned by varying the substituents in the naphthalimide system.[9]

In this work, a 4-styryl-1,8-naphthalimide chromophore possessing long wavelength fluorescence was used as the photoactive component.[10] Azadithia-15-crown-5-ether was chosen as a receptor unit, which, as we have shown previously,[11] demonstrates high selectivity towards mercury(II) cations in aqueous solutions. In the suggested chemosensor **1** (Scheme 1), the receptor group is incorporated into the electron-donating substituent located at position 4 of the naphthalimide system. The existence of conjugation between the nitrogen atom of the macrocycle and the carbonyl groups of the imide residue implied that spectral response should appear by the ICT-mechanism,[12] according to which complexation should cause changes in the energy of intramolecular charge transfer (ICT) electronic transition occurring in the chromophore upon photoexcitation. In particular, coordination of the cation on the crown ether moiety is assumed to hinder the shift of electron density from the receptor to the dicarboxyimide moiety and is accompanied by a blue shift of the absorption and fluorescence maxima. The choice of the *n*-butyl group as the substituent at the imide nitrogen atom was determined by the higher solubility of *N*-alkyl-1,8-naphthalimides in comparison with the corresponding *N*-aryl derivatives, which favors the purification of the compound and preparation of its solutions for studies of the sensor properties.

Chemosensor **1** was prepared by the Heck reaction between 4-bromo-*N*-butyl-1,8-naphthalimide **4** and crown-containing styrene **3** (see Scheme 1) by the procedure suggested previously for the reaction of **4** with 4-dimethylaminostyrene.[13] Intermediate **3** was synthesized from aldehyde **2** by the Wittig reaction under

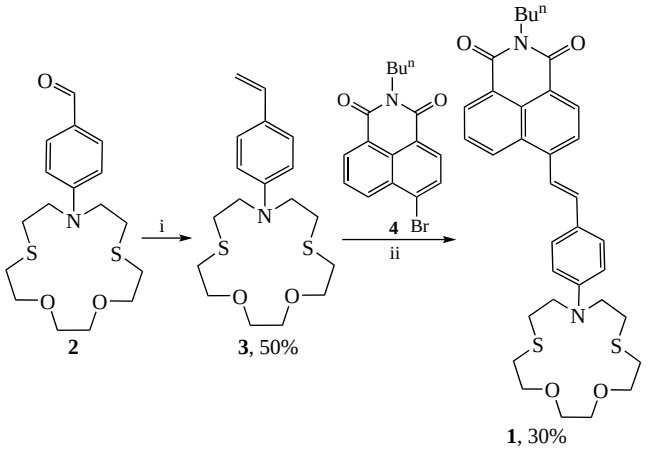

Scheme 1 *Reagents and conditions*: i, $[Ph_3PMe]^+I^-$, Bu^{t}OK, THF, room temperature; ii, $Pd(OAc)_2$, (*o*-Tol)$_3$P, Et_3N, DMF, 105 °C.

the conditions used in a synthesis of a structurally similar compound.[14] The intermediate 4-bromo-1,8-naphthalimide **4** and aldehyde **2** were prepared using reported methods.[15] Experimental details of the synthesis as well as data of physicochemical methods of analysis for compounds **1** and **3** are given in Online Supplementary Materials.

The long wavelength band in the absorption spectrum of **1** in water with a maximum at 490 nm [Figure 1(*a*)] corresponds to the intramolecular charge transfer from the donor nitrogen atom of the aryl moiety to the electron-acceptor carbonyl groups of the dicarboxyimide residue. The fluorescence of compound **1** is characterized by the presence of a band (quantum yield 0.028) around 680 nm [Figure 1(*b*)]. Addition of Hg^{2+} to an aqueous solution of **1** resulted in a new band shifted hypsochromically by 100 nm in the absorption spectrum, which is associated with the coordination of the mercury cation to the crown ether residue [see Figure 1(*a*)]. This seems to be due to the fact that upon complexation, the nitrogen atom of the macrocyclic moiety is partially disconnected from the conjugated system. Moreover, binding of the mercury cation by the crown ether receptor was confirmed using ^{1}H NMR spectroscopy. In the presence of

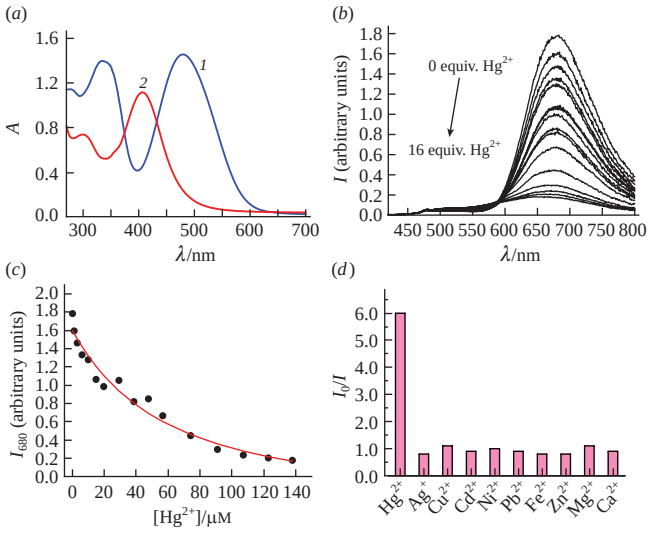

Figure 1 Spectral properties of compound **1** (10 μmol dm^{-3}) in water (pH 4.5, acetate buffer, 0.01 M). (*a*) Absorption spectrum of **1** in the absence (*1*) and in the presence (*2*) of mercury(II) perchlorate. (*b*) Fluorescence spectra of **1** upon gradual addition of $Hg(ClO_4)_2$, excitation wavelength 410 nm. (*c*) Dependence of fluorescence intensity of **1** at 680 nm (I_{680}) on the concentration of Hg^{2+} cations in solution (the points correspond to experimental data, while the curves, to the calculation). (*d*) Ratio of fluorescence intensity of **1** (I_0) to the intensity after addition of 10 equiv. of the metal cation (I) at 680 nm; excitation wavelength 410 nm.

mercury perchlorates, a strong downfield shift of the signals for the benzene protons and crown-ether ring protons was observed. The proton signals of the naphthalimide part were also shifted, but to a smaller extent (see Online Supplementary Materials, Figure S1).

Gradual addition of mercury cations resulted in quenching of the fluorescence of **1** in the fluorescence spectrum. The decrease in the intensity of the emission band may be due to the internal heavy atom effect in the complex formed.[16] The observed changes in the fluorescence emission spectrum [see Figure 1(*b*)] corresponded to the formation of a 1 : 1 complex. It was also found that the experimental data on the dependence of the signal intensity at a wavelength of 680 nm on the concentration of $Hg(ClO_4)_2$ comply with the results of theoretical calculations by the SpecFit32 program,[17] provided that only the formation of the complex with this composition is taken into account [Figure 1(*c*)]. Based on the data obtained by spectrofluorimetric titration, we determined the logarithm of the stability constant of (**1**)·Hg^{2+} (log*K*), which amounted to 4.25 ± 0.09. The lower value of log*K* for the (**1**)·Hg^{2+} compared to that obtained for the complex of the reported 4-acetylamino-1,8-naphthalimide with a similar *N*-phenylazadithia-15-crown ether receptor located in the CO–N(Ar)–CO fragment as Ar-group (log*K* = 6.51 ± 0.03)[11] could be a result of conjugation between the receptor's nitrogen atom lone pair and carbonyl groups in the molecule **1**.

To analyze the selectivity of sensor **1**, the fluorescent responses to the presence of various metal ions were measured. The ratio of the fluorescence intensity of the free ligand at 680 nm to the intensity at the same wavelength detected after the addition of a metal cation was used as a measure of the response. The data in Figure 1(*d*) show that addition of 10 equiv. of Hg^{2+} results in significant fluorescence quenching, while in the cases of Cu^{2+}, Ag^+, Zn^{2+}, Ni^{2+}, Pb^{2+}, Cd^{2+}, Ca^{2+}, Mg^{2+} and Fe^{2+} cations, the changes were insignificant.

In the next part of this work, we studied the possibility of using compound **1** for the fluorescent visualization of Hg^{2+} in living cells. Confocal laser scanning microscopy (CLSM) shows that **1** penetrates into HEK 293 cells. It is diffusely distributed in the cytoplasm and accumulated in submicron-sized vesicular structures [Figure S2(*a*),(*b*)]. It should be noted that the intracellular fluorescence spectrum of **1** is characterized by a shorter wavelength position of the maximum (600 nm in the cytoplasm and 567 nm in the vesicles, see Figure S2) compared to its spectrum in water [see Figure 1(*b*)]. Most likely, the blue shift upon going from the aqueous solution to the intracellular medium results from a decrease in the polarity of the styrylnaphthalimide fluorophore microenvironment.[13,18]

Comparison of the images of intracellular distribution of **1** in vesicular structures obtained by CLSM with the distribution of lipid droplets observed in the transmission images led to the conclusion that **1** accumulates in lipid droplets, cellular organelles that store neutral lipids (Figure S3). In this work, we showed that intracellular accumulation of **1** reached saturation within 2 h of incubation of HEK 293 cells with **1** (5 μM), while the half-accumulation time was 48 ± 1 min [Figure S4(*a*)]. When cells were incubated with compound **1** for 30 min, the intracellular concentration of the compound increased linearly with incubation concentrations of the sensor in the range of 1–20 μM [Figure S4(*b*)]. The pattern of intracellular distribution of the compound remains unchanged. The further increase in the incubation concentration of **1** is limited by the toxicity of the solubilizer. The kinetics of **1** elimination from HEK 293 cells showed that the intracellular concentration of the dye decreased by half in 49 ± 1 min after removal of the compound from the external environment. In the subsequent hours, a decrease in the rate of **1** excretion from cells was observed [see Figure S4(*a*)].

Thus, compound **1** is characterized by equal rates of cellular accumulation and excretion.

Pre-incubation of cells with $Hg(ClO_4)_2$ (5–100 μM, 30 min) followed by incubation of HEK 293 cells with **1** (5 μM, 30 min) did not change the qualitative picture of intracellular distribution of **1** and the shape of intracellular fluorescence spectra but decreased the intracellular fluorescence intensity of **1**, which, taking the results of studies of the sensor properties of **1** in an aqueous solution into account, indicates that a complex with the Hg^{2+} cation is formed (Figure 2). In the range of $Hg(ClO_4)_2$ concentrations studied (5–30 μM), the decrease in the intracellular fluorescence intensity of **1** occurs in proportion to the amount of Hg^{2+} [Figure 2(*d*)]. Raising the concentration of $Hg(ClO_4)_2$ in the extracellular medium above 80 μM does not decrease the intracellular fluorescence intensity of **1** considerably.

In summary, the optical response of styrylnaphthalimide **1** to the presence of mercury(II) cations involves a hypsochromic shift of the long wavelength absorption band and a decrease in the signal intensity in the emission spectrum associated with the formation of a non-fluorescent complex. Compound **1** can be used as a selective colorimetric and fluorescent chemosensor for Hg^{2+} ions in aqueous solutions and for the qualitative fluorimetric determination of this ion in living cells.

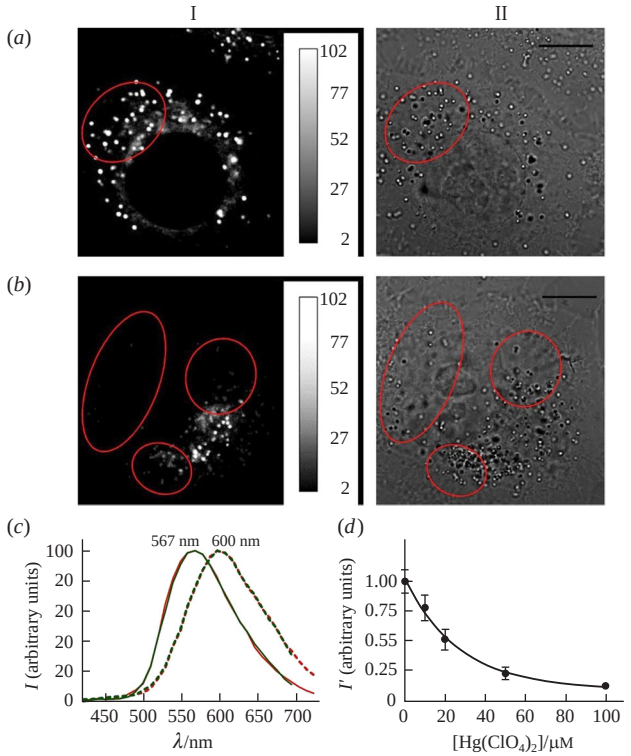

Figure 2 (*a*, *b*) Confocal fluorescence images and (*c*) fluorescence spectra of compound **1** and its complex with Hg^{2+} cations in HEK 293 cells at λ_{ex} = 405 nm. (*a*) Cells were incubated with **1** (5 μM, stock solution in DMSO) for 30 min. (*b*) Cells were pre-incubated for 30 min with 20 μM $Hg(ClO_4)_2$, washed twice with the Hanks' solution and incubated with 5 μM **1** for 30 min. Column I shows CLSM images of intracellular fluorescence in the spectral range of 510–730 nm. The fluorescence intensity scale is presented in relative units. Column II shows images of cells in transmitted light. The scale label is 5 μm. Ellipses indicate groups of lipid droplets located at the cell periphery and visible as bright white or black granules. (*c*) Typical normalized intracellular fluorescence spectra of **1** (green lines) and of the complex of **1** with Hg^{2+} (red lines) in lipid droplets (solid line) and in the cytoplasm (dashed line). (*d*) Dependence of the mean fluorescence intensity of **1** in HEK 293 cells (*I*′) on the concentration of $Hg(ClO_4)_2$. HEK 293 cells were pre-incubated with 5–100 μM $Hg(ClO_4)_2$ for 30 min, washed twice with the Hanks' solution and incubated for 30 min with 5 μM of **1** from a stock solution in DMSO. Data were averaged over 30 to 40 cells in each measurement and presented as the mean value per cell ±SD.

This work was supported by the Russian Science Foundation (grant no. 20-73-10186-P). Steady-state fluorescence spectroscopy studies were performed with financial support from the Ministry of Science and Higher Education of the Russian Federation using the equipment of the Center for molecular composition studies of INEOS RAS.

Online Supplementary Materials

Supplementary data associated with this article can be found in the online version at doi: 10.1016/j.mencom.2024.04.034.

References

1 (*a*) H. Fang, Y. Li, S. Yao, S. Geng, Y. Chen, Z. Guo and W. He, *Front. Pharmacol.*, 2022, **13**, 927609; (*b*) R. A. Festa and D. J. Thiele, *Curr. Biol.*, 2011, **21**, R877.
2 M. N. Rana, J. Tangpong and M. Rahman, *Toxicol. Rep.*, 2018, **5**, 704.
3 (*a*) L. Deng, Y. Li, X. Yan, J. Xiao, C. Ma, J. Zheng, S. Liu and R. Yang, *Anal. Chem.*, 2015, **87** 2452; (*b*) A. F. Castoldi, C. Johansson, N. Onishchenko, T. Coccini, E. Roda, M. Vahter, S. Ceccatelli and L. Manzo, *Regul. Toxicol. Pharmacol.*, 2008, **51**, 201.
4 H. H. Harris, I. J. Pickering and G. N. George, *Science*, 2003, **301**, 1203.
5 M. Harada and B. R. Von, *J. Appl. Toxicol.*, 1995, **15**, 483.
6 (*a*) K. M. Rice, E. M. Walker, Jr., M. Wu, C. Gillette and E. R. Blough, *J. Prev. Med. Public Health*, 2014, **47**, 74; (*b*) B. Fernandes Azevedo, L. Barros Furieri, F. M. Peçanha, G. A. Wiggers, P. Frizera Vassallo, M. Ronacher Simões, J. Fiorim, P. Rossi de Batista, M. Fioresi, L. Rossoni, I. Stefanon, M. J. Alonso, M. Salaices and D. V. Vassallo, *J. Biomed. Biotechnol.*, 2012, 949048.
7 (*a*) M. Bahta and N. Ahmed, *J. Photochem. Photobiol., A*, 2018, **357**, 41; (*b*) J. Hu, J. Li, J. Qi and J. Chen, *New J. Chem.*, 2015, **39**, 843.
8 (*a*) M. Bahta and N. Ahmed, *J. Photochem. Photobiol., A*, 2019, **373**, 154; (*b*) L. Chen, S. J. Park, D. Wu, H. Kim and J. Yoon, *Chem. Commun.*, 2019, **55**, 1766; (*c*) T. T. K. Cuc, P. Q. Nhien, T. M. Khang, H.-Y. Chen, C.-H. Wu, B. T. B. Hue, Y.-K. Li, J. I. Wu and H.-C. Lin, *Dyes Pigm.*, 2022, **197**, 109907; (*d*) P. A. Panchenko, P. A. Ignatov, M. A. Zakharko, Yu. V. Fedorov and O. A. Fedorova, *Mendeleev Commun.*, 2020, **30**, 55.
9 (*a*) S. L. Selector, L. B. Bogdanova, A. V. Shokurov, P. A. Panchenko, O. A. Fedorova and V. V. Arslanov, *Macroheterocycles/ Makrogeterotsikly*, 2014, **7**, 311; (*b*) O. A. Fedorova, A. N. Sergeeva, P. A. Panchenko, Y. V. Fedorov, F. G. Erko, J. Berthet and S. Delbaere, *J. Photochem. Photobiol., A*, 2015, **303**–**304**, 28; (*c*) P. A. Panchenko, A. N. Sergeeva, O. A. Fedorova, Y. V. Fedorov, R. I. Reshetnikov, A. E. Schelkunova, M. A. Grin and A. F. Mironov, *J. Photochem. Photobiol., B*, 2014, **133**, 140.
10 (*a*) S. Luo, J. Lin, J. Zhou, Y. Wang, X. Liu, Y. Huang, Z. Lu and C. Hu, *J. Mater. Chem. C*, 2015, **3**, 5259; (*b*) J. Sun and Y. Qian, *Chin. J. Org. Chem.*, 2015, **35**, 1104; (*c*) K. Chen, Z. Gao, J. Sun, X. Hou and J. Chen, *Chem. Commun.*, 2020, **56**, 13037; (*d*) A. N. Arkhipova, P. A. Panchenko, Y. V. Fedorov and O. A. Fedorova, *Mendeleev Commun.*, 2017, **27**, 53.
11 P. A. Panchenko, A. S. Polyakova, Yu. V. Fedorov and O. A. Fedorova, *Russ. Chem. Bull.*, 2021, **70**, 1939.
12 S. Enbanathan and S. K. Iyer, *Ecotoxicol. Environ. Safety*, 2022, **247**, 114272.
13 P. A. Panchenko, A. N. Arkhipova, O. A. Fedorova, Y. V. Fedorov, M. A. Zakharko, D. E. Arkhipov and G. Jonusauskas, *Phys. Chem. Chem. Phys.*, 2017, **19**, 1244.
14 Q. Lin, L. Yang, Z. Wang, Y. Hua, D. Zhang, B. Bao, C. Bao, X. Gong and L. Zhu, *Angew. Chem.*, 2018, **130**, 3784.
15 (*a*) K. G. Leslie, D. Jacquemin, E. J. New and K. A. Jolliffe, *Chem. – Eur. J.*, 2018, **24**, 5569; (*b*) H. Lv, G. Yuan, G. Zhang, Z. Ren, H. He, Q. Sun, X. Zhang and S. Wang, *Dyes Pigm.*, 2020, **172**, 107658.
16 (*a*) C. Wu, J.-L. Zhao, X.-K. Jiang, C.-Z. Wang, X.-L. Ni, X. Zeng, C. Redshaw and T. Yamato, *Dalton Trans.*, 2016, **45**, 14948; (*b*) X.-L. Ni, Y. Wu, C. Redshaw and T. Yamato, *Dalton Trans.*, 2014, **43**, 12633; (*c*) H. Mu, R. Gong, Q. Ma, Y. Sun and E. Fu, *Tetrahedron Lett.*, 2007, **48**, 5525.
17 S. D. Tokarev, A. Botezatu, A. V. Khoroshutin, Yu. V. Fedorov and O. A. Fedorova, *Mendeleev Commun.*, 2022, **32**, 367.
18 A. S. Efimova, M. A. Ustimova, M. A. Maksimova, A. Yu. Frolova, V. I. Martynov, S. M. Deyev, A. A. Pakhomov, Yu. V. Fedorov and O. A. Fedorova, *Mendeleev Commun.*, 2023, **33**, 384.

Received: 19th January 2024; Com. 24/7377